

Visualization and Analysis of Large-Scale Atomistic Simulations of Plasma–Surface Interactions

Wathsala Widanagamaachchi,¹ Karl Hammond,² Li-Ta Lo,³ Brian Wirth,⁴ Francesca Samsel,⁵
Christopher Sewell,³ James Ahrens,³ and Valerio Pascucci¹

¹Scientific Computing and Imaging Institute, University of Utah, Salt Lake City, UT 84122

²Department of Chemical Engineering, University of Missouri, Columbia, MO 65211

³Los Alamos National Laboratory, Los Alamos, NM 87545

⁴Department of Nuclear Engineering, University of Tennessee, Knoxville, TN 37996

⁵University of Texas at Austin, Austin, TX 78712

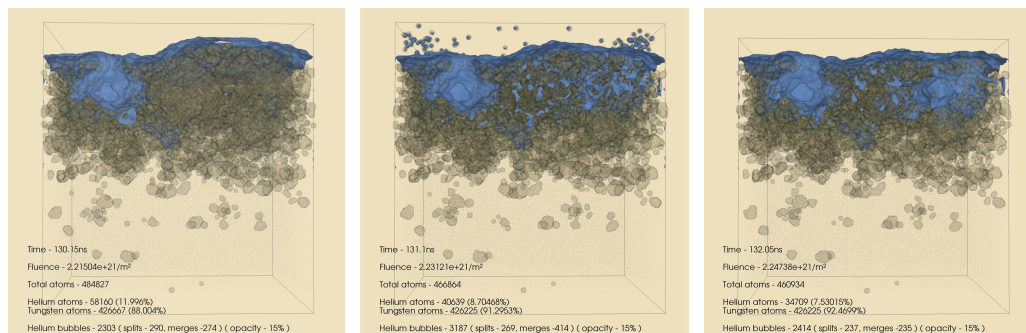


Figure 1: Snapshots around a time the tungsten surface is pushed upward by a over-pressurized helium bubble (left), then recoils as the bubble bursts (center, right). In each snapshot, the tungsten voids are indicated in blue, helium bubbles in gray, and the extracted statistics and bubble evaluation details are also displayed. Here, the simulation box is ≈ 20 nm wide.

Abstract

We present a simulation–visualization pipeline that uses the LAMMPS Molecular Dynamics Simulator and the Visualization Toolkit to create a visualization and analysis environment for atomistic simulations of plasma–surface interactions. These simulations are used to understand the origin of fuzz-like, microscopic damage to tungsten and other metal surfaces by helium. The proposed pipeline serves both as an aid to visualization, i.e. drawing the surfaces of gas bubbles and voids/cavities in the metal, as well as a means of analysis, i.e. extracting various statistics and gas bubble evolution details. The result is a better understanding of the void and bubble formation process that is difficult if not impossible to get using conventional atomistic visualization software.

Categories and Subject Descriptors (according to ACM CCS): J.2 [Computer Applications]: Physical Sciences and Engineering—Physics I.6.4 [SIMULATION AND MODELING]: Model Validation and Analysis—

1. Introduction

As the computing power and storage capacity of supercomputers grow, scientists gain the ability to simulate complex phenomena with ever-increasing resolution. However, the

rate at which these simulations generate data severely taxes the existing analysis and visualization tasks. In addition, it is sometimes non-trivial to understand what is actually happening in traditional visualizations, as parts of the simulation

the user considers “interesting” are obscured by other parts of the simulation.

Simulations of plasma–surface interactions have recently been the focus of significant research due to interest in the origin of fuzz-like, microscopic damage to tungsten and other metal surfaces by helium as seen experimentally [BD08, KSO*09]. Such simulations have shown that helium spontaneously aggregates to form clusters and eventually bubbles, pushing out tungsten surface defects, i.e. voids/cavities, in the process [ZWLH13, ZWHD14, SHJW13]. There are many challenges to these types of simulations. First, the length scale of atomistic simulations is typically on the order of 1–10 nm; large simulations such as those we discuss here may reach 20, 50, or 100 nm on a side, resulting in $\mathcal{O}(10^6\text{--}10^7)$ atoms per simulation. The second problem is that the time step required is typically $\mathcal{O}(10^{-16}$ s), meaning that a simulation one microsecond long takes on the order of several months to several years to complete. This problem is also compounded by the fact that simulations of tungsten plasma exposure at realistic flux require even larger systems: it is typically impossible or impractical to allow significantly more time between helium bombardments, so the alternative is to increase the area of the simulation, and thus the number of atoms.

Another challenge is what to do with the data we collect. Simply looking at the atoms tells us something, but in this sort of simulation, it is almost more interesting to know where the atoms are *not*, that is, where voids have been created in the material due to burst helium bubbles. See, for example, the work of Sefta et al. [SHJW13, SJW13] and Zhang et al. [ZWLH13]. In this case, we are interested in the position of something that *isn't there*. This motivates a type of visualization that is not purely based on atomic positions (or lack thereof), but on the *boundaries* between different domains, e.g. metal, void, and bubble. Conventional atomistic visualizations [Stu10, LBH12, PSA13, GKM*14] fail to provide sufficient information for understanding this bubble and void formation process. In molecular visualizations [KRS*13, LBBH13, PTRV13, LBH14], some relevant research can be found on visualizing and tracking empty spatial regions in data. In contrast to these, our goal here is to identify and visualize these bubbles and voids in such a manner that the resulting simulation–visualization pipeline can be used in an in-situ environment (once the necessary parallelization is achieved).

The rest of this article discusses our simulation–visualization scheme for large-scale atomistic simulations of plasma-facing materials. The visualization phase identifies the boundaries between helium-filled regions, tungsten-filled regions, and voids, using an algorithm encoded through library calls to the Visualization Toolkit (VTK) [SML06]. Several atom statistics and helium bubble evolution details are identified during the analysis phase through calls to the Large-scale Atomic/Molecular Mas-

sively Parallel Simulator (LAMMPS) [Pl95]. The resulting visualizations provide additional insights into the process of void and bubble formation in plasma-facing materials. Here, we demonstrate the utility of our approach using a simulation containing $\approx 460,000$ atoms.

2. LAMMPS–VTK Pipeline

Here, we employ a tightly-coupled simulation–visualization strategy which allows us to collocate the simulation and visualization/analysis phases of the work. Specifically, the simulation itself is written as a “driver” program, which is then linked to LAMMPS via its library interface and to the VTK library. The simulation is periodically paused to insert helium as described by Hammond and Wirth [HW14], and every so often during one of these “breaks”, the visualization and analysis steps are executed without any significant disruption to the simulation or a need to export position/velocity data to disk.

As described in the previous paragraph, there is no limitation within the design of the pipeline to carry out both simulation and visualization/analysis steps in an in-situ environment. At present, the simulation data for the pipeline can either be extracted directly from LAMMPS in-situ, or loaded from dump files through LAMMPS or a VTK reader. However, as a scalable in-situ solution has not been achieved yet, for the specific examples given within this paper, the simulation is executed in a separate pre-processing step and a dump file with atom details is produced at each of these “breaks.” These dump files are later used to re-create the simulation state within the LAMMPS–VTK pipeline, and then the visualization and analysis steps are executed.

2.1. Simulation

The data used within this work are derived from a simulation of helium-irradiated tungsten at 933 K under relatively high-flux conditions ($\Gamma = 1.7 \times 10^{28}$ He/m²/s, including reflected ions). The simulation uses approximately the same flux as that used by Sefta et al. [SHJW13], which is $\mathcal{O}(10^5)$ higher than typical experimental fluxes [BD08] for reasons of tractability. Here, the simulation box is ≈ 20 nm on a side in the x - and y -directions, in which periodic boundary conditions are applied. The z -direction is a free surface, with the tungsten block being ≈ 16 nm deep.

During the simulation, helium atoms are inserted at random positions in the x – y plane with depths sampled from the depth distribution as described by Hammond and Wirth [HW14]. The potential energy due to tungsten–tungsten interactions is modeled by the Embedded Atom Method (EAM) potential of Finnis and Sinclair [FS84], as modified at short distances by Ackland and Thetford [AT87] and by Juslin and Wirth [JW13]. The tungsten–helium interactions are given by the pair potential of Juslin and Wirth [JW13], and helium–helium interactions are taken

from the pair potential of Beck [Bec68], as modified at short range by Morishita et al. [MSWD03]. Then the simulation undergoes 328,000 helium implantations, corresponding to a fluence, i.e. ions per unit area, of $\Phi = 2.7 \times 10^{21}$ He/m² (including ions that reflect and therefore do not implant), and is visualized every 1000 insertions as detailed in the next section.

2.2. Visualization

During the visualization phase, boundaries between helium-filled regions, tungsten-filled regions, and tungsten voids are identified and visualized through library calls to VTK. As a first step, helium atoms are separated from tungsten atoms using the *vtkThresholdPoints* filter. To identify the boundaries between helium-filled regions, a Gaussian density is first created around each helium atom and later an isosurface is extracted around each helium bubble. Here, the *vtkFastSplatter* subroutine is used to place a Gaussian function at the coordinates of each helium atom. The splat image for the *vtkFastSplatter* call is constructed using *vtkImageGaussianSource* to instruct VTK to create the resampling density from a Gaussian function. The radius of this splat image is set to be one lattice unit ($a \approx 3.177$ Å), as that distance is just larger than the tungsten–helium cutoff distance with this potential. This enables the *vtkFastSplatter* subroutine to construct a “density” of helium atoms, which is later used for drawing the “surface” of a helium bubble. In drawing an isosurface around each bubble, the *vtkContourFilter* subroutine is used with isovalue 0.5.

To visualize tungsten voids, Gaussian functions are placed at the positions of all atoms, including helium (that way, the helium atoms also create a Gaussian density on themselves, thereby eliminating spurious voids that are actually bubbles). Here, again, the *vtkFastSplatter* and *vtkImageGaussianSource* subroutines are used. The radius of the splat images is set to be one lattice unit, though there is less motivation behind this choice: the nearest-neighbor tungsten–tungsten distance ($\sqrt{3}a/2 \approx 2.75$ Å) would likely yield similar results. Then, the *vtkContourFilter* subroutine is again used with isovalue 0.5 to extract the isosurface around the atoms. Since we are only interested in seeing the tungsten voids inside the simulation box, and because VTK has no concept of periodic boundary conditions (which are present in the *x*- and *y*-directions), the subroutine *vtkClipPolyData* is then used to clip the spurious “shell” around the simulation box. Furthermore, we utilize several color maps to visualize these data effectively (Figure 2) and camera movement is also enabled during the course of the visualization. Additional functionality such as automatic translation and movement of the camera toward salient regions within the simulation are still being investigated.

In order to extend our work to provide large-scale parallel visualization for the in-situ application, all VTK fil-

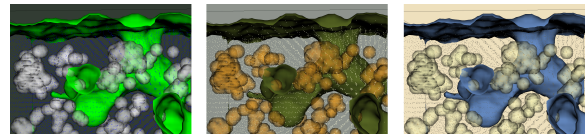


Figure 2: Simulation data from Sefta [Sef13] visualized using different color maps. Using the rightmost image as a guide, the gray/white regions are helium bubbles, while the blue regions are tungsten surfaces, thus voids, external surface. Here, the simulation box is 6.35 nm wide and contains $\approx 25,000$ atoms.

ters used in our pipeline must be made to function across a distributed domain decomposition. While the *vtkContourFilter* already supports this, we will need to parallelize the serial VTK splatting filters. Each rank will require access to all atoms which contribute to the density within its domain, including atoms located outside its domain but within the splat radius. In the case that the splat radius is no larger than the force cut-off distance for the potential used by the physics computations in LAMMPS, the necessary atoms will already be available locally to the in-situ visualization because they are in the ghost zones maintained by the simulation itself. However, to handle cases in which the splat radius is larger than the force cut-off distance, we would need to communicate additional atoms between ranks. One convenient option for implementing this communication would be to use the latest version of the Do-It-Yourself library (DIY2) [PRK*11], which provides commonly used distributed communication patterns such as this.

2.3. Analysis

In addition to visualization, obtaining quick analysis details about the data is also of interest to the domain scientists. Here, we incorporated several statistics, such as fluence, atomic percentage of helium and tungsten atoms, and number of helium bubbles into the analysis phase. Furthermore, with the use of a volume overlap metric to determine correlations across time, the evolution details of helium bubbles, i.e. how they split and/or merge over time, are also identified and the number of splits and merges are extracted.

We are still exploring efficient means of conveying these evolution details within the visualization, e.g. coloring the bubbles by size, selecting color maps which can adeptly convey evolution details etc. An example showing the evolution of a single helium bubble growing over time, with the bubbles color-coded by size, is shown in Figure 3. Within this work, the evolution details of helium bubbles are only displayed along with the statistics, as shown in Figure 1. In a post-processing step, using the work of [WCBP12] we manage to visualize these evolution details (Figure 4) and enable scientists to understand the evolution details of helium bubbles by exploring its parameter range.

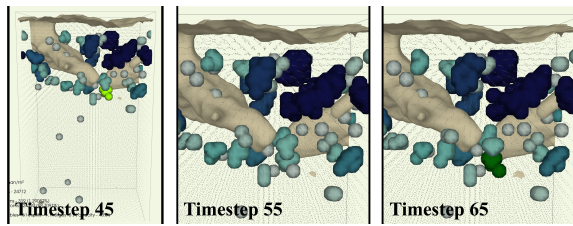


Figure 3: Snapshots around the time a helium bubble splits to form two small bubbles (left), then merges back into one bubble again (right). Here, the split bubbles are colored light green, while the merged bubble is colored dark green. Other helium bubbles are colored using a blue color map, with darker, bluer colors indicating larger bubbles and lighter blue colors indicating smaller bubbles. Here, the simulation box is 6.35 nm wide and contains $\approx 25,000$ atoms. Simulation data from Sefra [Sef13].

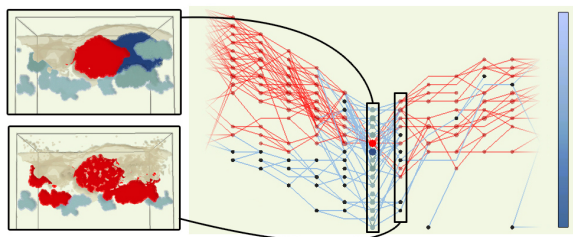


Figure 4: A tracking graph [WCBP12] (right) visualizing the evolution of helium bubbles around the time one helium bubble bursts, same as in Figure 1. Within the graph, each set of nodes in a vertical column represents helium bubbles in one timestep and their evolution are shown as a collection of feature tracks that merge and/or split. The top left and bottom left images visualize the helium bubbles (color-coded by size using a blue color map) and tungsten voids (in beige) for two timesteps. The bubble that bursts and its evolution is highlighted in ‘red’. For simplicity, only bubbles with $\text{size} > 500$ atoms are visualized.

3. Results

A representative result of applying our visualization/analysis scheme to a simulation of the surface of a plasma-facing component (containing $\approx 460,000$ atoms) is shown in Figure 1. This particular set of snapshots shows the event of a helium-filled bubble bursting as the tungsten ‘‘ligament’’ shielding it from the surface thins to the point of rupture. Compared to traditional atomistic visualizations which use atomic positions and spheres, the resulting void is easily seen here. Due to the semi-transparent shading scheme, we can clearly see the surface ‘‘bulge’’ due to the over-pressurized bubble and then recoil right after the bubble bursts.

The accompanying movie shows a simulation of roughly 150 ns of real time, starting with a pristine, undamaged tung-

sten surface, as helium is implanted below the surface every 0.475 ps (at a flux of $\Gamma = 1.7 \times 10^{28}$ He/m²/s). Throughout the simulation, the interstitial helium atoms migrate within the BCC tungsten matrix with very high mobility. The injected helium atoms thus rapidly diffuse in more or less random trajectories that can result in returning to the free surface and escaping, or diffusing deeper into the solid until they encounter a defect or another helium atom or group of helium atoms. Due to the essentially repulsive nature of the helium–tungsten interactions, the helium has a strong driving force to cluster (in order to minimize the number and strength of repulsive tungsten–helium forces). Any clusters that form continue to undergo an essentially random walk with high diffusivity.

As the migrating helium clusters grow larger, they eventually reach a condition in which the stress created is sufficient to create a tungsten vacancy and self-interstitial (Frenkel) pair, a process called trap mutation [SJW13, HHWM14]. The size at which trap mutation first occurs depends on a number of factors, including the temperature and the proximity of the helium cluster to the free surface, as well as the surface orientation [HW14, HHWM14]. The resulting helium–vacancy clusters, which contain multiple helium atoms, serve as nuclei for helium bubbles at higher fluence. These bubbles grow through the absorption of mobile helium atoms and clusters during continued plasma exposure. The gas bubbles continue to increase in pressure through absorption of mobile helium until the pressure reaches the level required for dislocation loop punching [PVU14, SHJW13]. The punching of prismatic dislocation loops allows the gas bubbles to increase in volume, thereby reducing pressure.

The final process observed in atomistic simulations is the rupture of over-pressurized helium gas bubbles that are near the surface. This process is easily observed through visualization processes such as the one discussed here (Figure 1). In some cases, it is even possible to see bubbles rupture, their surface ligaments subsequently re-form, and then fill with helium again. This type of visualization has the capability of providing very different kinds of analyses than traditional atomistic visualization, and it provides something traditional atomistic visualizers cannot easily do: show us where the atoms *aren’t*.

4. Conclusion

In this paper, we present a tightly-coupled simulation–visualization strategy for large-scale atomistic simulations of plasma-facing materials. The proposed pipeline enables both visualization, i.e. drawing the surfaces of gas bubbles and voids in the metal, and analysis, i.e. extracting fluence, atom statistics and gas bubble evolution details of data. The resulting visualizations, as demonstrated, are capable of providing additional insights into the process of void and bubble formation compared to traditional atomistic visualizations.

Acknowledgments

This material is based upon work supported by the U.S. Department of Energy, Office of Science, Office of Advanced Scientific Computing Research, Scientific Discovery through Advanced Computing (SciDAC) program, through the SDAV Institute. Primary financial support for this work was provided through the Scientific Discovery through Advanced Computing (SciDAC) project on Plasma–Surface Interactions, funded by the U. S. Department of Energy, Office of Science, Advanced Computing Research, and Fusion Energy Sciences under award DE–SC00–08875. Additional funding was provided through the Plasma–Surface Interactions Science Center, funded by the U. S. Department of Energy, Office of Fusion Energy Sciences under award DE–SC00–02060.

Significant computing resources were used by this project at the National Energy Research Scientific Computing (NERSC) facility at Lawrence Berkeley National Laboratory and at the Argonne Leadership Computing Facility (ALCF) at Argonne National Laboratory, which are supported by the Office of Science of the U. S. Department of Energy under contracts DE–AC02–06CH11231 and DE–AC02–06CH11357, respectively.

Work performed on this paper was completed while the last author was on sabbatical at the King Abdullah University of Science and Technology. The authors acknowledge logistical and computational support from KAUST.

References

- [AT87] ACKLAND G. J., THETFORD R.: An improved N -body semi-empirical model for b.c.c transition metals. *Philos. Mag. A* 56 (1987), 15–30. 2
- [BD08] BALDWIN M. J., DOERNER R. P.: Helium induced nanoscopic morphology on tungsten under fusion relevant plasma conditions. *Nucl. Fusion* 48 (2008), 035001. 2
- [Bec68] BECK D. E.: A new interatomic potential function for helium. *Mol. Phys.* 14 (1968), 311–315. *Ibid.* vol. 15, no. 4, p. 332, 1968. 3
- [FS84] FINNIS M. W., SINCLAIR J. E.: A simple empirical N -body potential for transition metals. *Philos. Mag. A* 50 (1984), 45–55. 2
- [GKM*14] GROTTTEL S., KRONE M., MULLER C., REINA G., ERTL T.: Megamol—a prototyping framework for particle-based visualization. 2
- [HHWM14] HU L., HAMMOND K. D., WIRTH B. D., MAROUDAS D.: Dynamics of small mobile helium clusters near tungsten surfaces. *Surf. Sci.* 626 (2014), L21–L25. 4
- [HW14] HAMMOND K. D., WIRTH B. D.: Crystal orientation effects on helium ion depth distributions and adatom formation processes in plasma-facing tungsten. *J. Appl. Phys.* 116 (2014), 143301. 2, 4
- [JW13] JUSLIN N., WIRTH B. D.: Interatomic potentials for simulation of He bubble formation in W. *J. Nucl. Mater.* 432 (2013), 61–66. 2
- [KRS*13] KRONE M., REINA G., SCHULZ C., KULSCHEWSKI T., PLEISS J., ERTL T.: Interactive extraction and tracking of biomolecular surface features. In *Computer Graphics Forum* (2013), vol. 32, Wiley Online Library, pp. 331–340. 2
- [KSO*09] KAJITA S., SAKAGUCHI W., OHNO N., YOSHIDA N., SAEKI T.: Formation process of tungsten nanostructure by the exposure to helium plasma under fusion relevant plasma conditions. *Nucl. Fusion* 49 (2009), 095005. 2
- [LBBH13] LINDOW N., BAUM D., BONDAR A.-N., HEGE H.-C.: Exploring cavity dynamics in biomolecular systems. *BMC bioinformatics* 14, Suppl 19 (2013), S5. 2
- [LBH12] LINDOW N., BAUM D., HEGE H.-C.: Interactive rendering of materials and biological structures on atomic and nanoscopic scale. In *Computer Graphics Forum* (2012), vol. 31, Wiley Online Library, pp. 1325–1334. 2
- [LBH14] LINDOW N., BAUM D., HEGE H.: Ligand excluded surface: A new type of molecular surface. 2
- [MSWD03] MORISHITA K., SUGANO R., WIRTH B. D., DIAZ DE LA RUBIA T.: Thermal stability of helium–vacancy clusters in iron. *Nucl. Instrum. Meth. Phys. Res. B* 202 (2003), 76–81. 3
- [Pli95] PLIMPTON S. J.: Fast parallel algorithms for short-range molecular dynamics. *J. Comput. Phys.* 117 (1995), 1–19. <http://lammps.sandia.gov/>. 2
- [PRK*11] PETERKA T., ROSS R., KENDALL W., GYULASSY A., PASCUCCI V., SHEN H.-W., LEE T.-Y., CHAUDHURI A.: Scalable parallel building blocks for custom data analysis. In *Proceedings of Large Data Analysis and Visualization Symposium LDAV'11* (Providence, RI, 2011). 3
- [PSA13] PELED D., SILVERMAN A., ADLER J.: 3d visualization of atomistic simulations on every desktop. In *Journal of Physics: Conference Series* (2013), vol. 454, IOP Publishing, p. 012076. 2
- [PTRV13] PARULEK J., TURKAY C., REUTER N., VIOLA I.: Visual cavity analysis in molecular simulations. *BMC bioinformatics* 14, Suppl 19 (2013), S4. 2
- [PVU14] PEREZ D., VOGEL T., UBERUAGA B. P.: Diffusion and transformation kinetics of small helium clusters in bulk tungsten. *Phys. Rev. B* 90 (2014), 014102. 4
- [Sef13] SEFTA F.: *Surface Response of Tungsten to Helium and Hydrogen Plasma Flux as a Function of Temperature and Incident Kinetic Energy*. PhD dissertation, University of California, Berkeley, 2013. 3, 4
- [SHJW13] SEFTA F., HAMMOND K. D., JUSLIN N., WIRTH B. D.: Tungsten surface evolution by helium bubble nucleation, growth, and rupture. *Nucl. Fusion* 53 (2013), 073015. 2, 4
- [SJW13] SEFTA F., JUSLIN N., WIRTH B. D.: Helium bubble bursting in tungsten. *J. Appl. Phys.* 114 (2013), 243518. 2, 4
- [SML06] SCHROEDER W., MARTIN K., LORENSEN B.: *Visualization Toolkit: An Object-Oriented Approach to 3D Graphics*, fourth ed. Kitware, Inc., New York, 2006. 2
- [Stu10] STUKOWSKI A.: Visualization and analysis of atomistic simulation data with OVITO—the Open Visualization Tool. *Model. Simulat. Mater. Sci. Eng.* 18 (2010), 015012. 2
- [WCBP12] WIDANAGAMAACHCHI W., CHRISTENSEN C., BREMER P.-T., PASCUCCI V.: Interactive exploration of large-scale time-varying data using dynamic tracking graphs. In *LDAV* (2012), IEEE, pp. 9–17. 3, 4
- [ZWHD14] ZHOU Y. L., WANG J., HOU Q., DENG A. H.: Molecular dynamics simulations of the diffusion and coalescence of helium in tungsten. *J. Nucl. Mater.* 446 (2014), 49–55. 2
- [ZWLH13] ZHANG B. L., WANG J., LI M., HOU Q.: A molecular dynamics study of helium bubble formation and gas release near titanium surfaces. *J. Nucl. Mater.* 438 (2013), 178–182. 2